Modeling of hysteretic Schottky diode-like conduction in $Pt/BiFeO_3/SrRuO_3$ switches

E. Miranda, D. Jiménez, A. Tsurumaki-Fukuchi, J. Blasco, H. Yamada, J. Suñé, and A. Sawa

Citation: Appl. Phys. Lett. **105**, 082904 (2014);
View online: https://doi.org/10.1063/1.4894116
View Table of Contents: http://aip.scitation.org/toc/apl/105/8
Published by the American Institute of Physics

Modeling of hysteretic Schottky diode-like conduction in $Pt/BiFeO_3/SrRuO_3$ switches

E. Miranda,[1,a)] D. Jiménez,[1] A. Tsurumaki-Fukuchi,[2] J. Blasco,[1] H. Yamada,[2,3] J. Suñé,[1] and A. Sawa[2]

[1]*Departament d'Enginyeria Electrònica, Universitat Autònoma de Barcelona, 08193 Cerdanyola del Valles, Barcelona, Spain*

[2]*National Institute of Advanced Industrial Science and Technology (AIST), Tsukuba, Ibaraki 305-8562, Japan*

[3]*JST, PRESTO, Kawaguchi, Saitama 332-0012, Japan*

(Received 22 July 2014; accepted 16 August 2014; published online 26 August 2014)

The hysteresis current-voltage (*I-V*) loops in $Pt/BiFeO_3/SrRuO_3$ structures are simulated using a Schottky diode-like conduction model with sigmoidally varying parameters, including series resistance correction and barrier lowering. The evolution of the system is represented by a vector in a 3D parameter space describing a closed trajectory with stationary states. It is shown that the hysteretic behavior is not only the result of a Schottky barrier height (SBH) variation arising from the $BiFeO_3$ polarization reversal but also a consequence of the potential drop distribution across the device. The SBH modulation is found to be remarkably lower (<0.07 eV) than previously reported (>0.5 eV). It is also shown that the p-type semiconducting nature of $BiFeO_3$ can explain the large ideality factors (>6) required to simulate the *I-V* curves as well as the highly asymmetric set and reset voltages (4.7 V and -1.9 V) exhibited by our devices. © *2014 AIP Publishing LLC*. [http://dx.doi.org/10.1063/1.4894116]

Recent studies pursued in the field of resistive switching point out the $Pt/BiFeO_3$(BFO)/$SrRuO_3$(SRO) system as a promising candidate for advanced ferroelectric-based nonvolatile memory devices.[1–10] These structures exhibit rectifying and tunable conduction characteristics, do not require electroforming, and show high endurance ($>10^5$ cycles) and data retention ($>10^5$ s) at room temperature.[5,6] In defining the ON (high current) and OFF (low current) conduction states, these switches take advantage of the polarization reversal property exhibited by the multiferroic BFO film when subjected to opposite electric fields.[6,7] Although the connection between the orientation of the ferroelectric domains and conduction is well known, there are still many specific aspects of the electron transport mechanism that require a deeper investigation.[2,8] Several models have been proposed to the date to account for the *I-V* characteristics of these devices, mainly space charge limited conduction, Poole-Frenkel, Fowler-Nordheim, and Schottky-like conduction, but no consensus on which is the dominant mechanism has been reached yet.[10] In this letter, a compact representation for the minor and major *I-V* loops in Pt/BFO/SRO structures based on a Schottky diode-like conduction model in combination with sigmoidally varying parameters is explored. It is shown that the Schottky barrier height (SBH) modulation cannot explain by itself the large hysteretic loops and the remarkable asymmetry of the average coercive voltages. We found that the large band gap of BFO plays a crucial role in this connection. In addition, thanks to the well-behaved rectifying characteristics of our devices, a precise value of the SBH modulation is provided.

The devices under investigation are Au/Pt/BFO/SRO structures fabricated onto $SrTiO_3$ (STO) substrates. A 50 nm-thick SRO bottom electrode was grown on the substrate prior to a pulsed laser-deposited BFO layer (100 nm-thick). Both the BFO and SRO layers are epitaxially grown. An Au(100 nm)/Pt(10 nm) top electrode is deposited on the BFO layer through a shadow mask (100 μm × 100 μm) by E-beam evaporation. In order to control the Bi content, the BFO films are deposited from source targets with controlled Bi/Fe ratio. The Bi/Fe ratio in the film was estimated to be 0.76 ± 0.05 by inductively coupled plasma atomic emission spectroscopy. Details about the fabrication and characterization of the Bi-deficient BFO films, together with a confirmation of their ferroelectricity and p-type semiconducting nature can be found in Refs. 6 and 7. The *I-V* characteristics were measured with the top electrode (Au) grounded.

According to previous reports,[6,11–13] the *I-V* characteristic of a metal-ferroelectric contact is given by a Schottky diode-like expression

$$I(V) = AA^*T^2 \exp(-\phi_B/kT)\{\exp[eV_B/nkT] - 1\}, \quad (1)$$

where A is the conducting area, $A^* = 4\pi e m^* k^2/h^3$ the effective Richardson constant, T the temperature, m^* the electron/hole effective mass, e the electron charge, k the Boltzmann constant, and h the Planck constant. ϕ_B is the effective barrier height (see Fig. 1(a)), V_B the voltage drop across the Pt/BFO junction barrier and n the so-called ideality factor. Assuming a first order barrier lowering effect for reverse biases ($V < 0$),[14] ϕ_B can be expressed as

$$\phi_B = \phi + \beta V H(-V), \quad (2)$$

where ϕ is the SBH, $\beta > 0$ a constant, and H the Heaviside function: $H(x \geq 0) = 1$, $H(x < 0) = 0$. A series resistance (R_S) correction for the barrier voltage V_B is also considered[2]

$$V_B = V - IR_S. \quad (3)$$

[a)]Author to whom correspondence should be addressed. Electronic mail: enrique.miranda@uab.cat

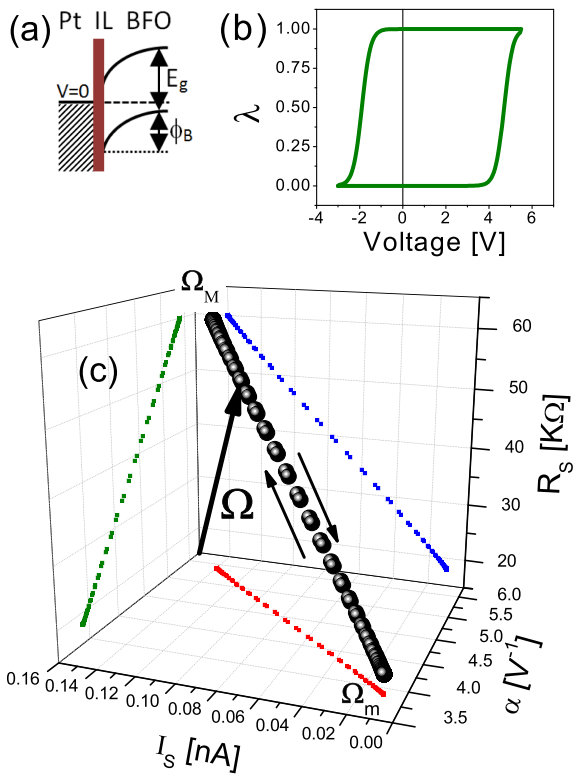

FIG. 1. (a) Schematic of the Pt/BFO barrier including an interfacial layer. (b) Plot of the fraction of polarized domains as a function of the applied voltage. (c) System trajectory in the parameter space. Ω_M and Ω_m are the stationary states corresponding to the ON and OFF current levels, respectively.

For typical parameter values of a rectifying structure, this effect is only significative for large positive bias ($V \gg 0$). The fraction of downward polarized domains $0 \leq \lambda \leq 1$ as a function of the applied bias is modelled according to the sigmoidal expression

$$\lambda(V) = 1/\{1 + \exp[-r(V - V_S H(\dot{V}) - V_R H(-\dot{V}))]\}, \quad (4)$$

where r is the switching rate, V_S the set voltage, V_R the reset voltage, and $\dot{V}$ the time derivative of V (see Fig. 1(b)). It can be demonstrated that assuming a box-type hysteretic model for a single ferroelectric or magnetic domain, the derivative of λ yields approximately the Gaussian distribution of coercive voltages around V_S and V_R associated with multiple domains.[15] Using (4), the state of the system is described by the vector $\Omega = (I_S, \alpha, R_S)$ which can be represented in a 3D space by the parametric equation

$$\Omega = \Omega_m + \lambda(\Omega_M - \Omega_m), \quad (5)$$

where $I_S = AA^*T^2\exp(-\phi/kT)$ and $\alpha = e/nkT$. $\Omega_m = (I_{Sm}, \alpha_m, R_{Sm})$ and $\Omega_M = (I_{SM}, \alpha_M, R_{SM})$ are the end points of the line segment shown in Fig. 1(c). To circumvent the uncertainties both in A^* (because of m^*) and A (because of SBH inhomogeneities),[13] we consider within this approach I_S instead of ϕ as one of the relevant descriptors of the hysteresis loop. The solution of the implicit equation (1) is given by the compact expression[16]

$$I(V) \approx (1/\alpha R_S)W\{\alpha R_S I_S \exp[\alpha(V + R_S I_S \exp[-\kappa V H(-V)]) - \kappa V H(-V)]\} - I_S \exp[-\kappa V H(-V)], \quad (6)$$

where $\kappa = \beta/kT$ and W is the Lambert function. The equality in Eq. (6) strictly holds for the stationary ON (Ω_M) and OFF (Ω_m) states. Figures 2(a) and 2(b) show typical major hysteresis I-V loops obtained by the application of double voltage sweeps in the range $-3\,\text{V} \rightarrow +5\,\text{V} \rightarrow -3\,\text{V}$. The curve illustrated in Figure 2(a) corresponds to a fresh device, whereas the curve shown in Figure 2(b) corresponds to a highly cycled device. The solid lines were calculated using Eq. (6). The agreement is very good but it is evident that Eq. (3) is a very simplistic approximation. R_s, which represents the resistance of the BFO layer, might be a function of the voltage or the current as well. Notice also that the possible role played by the dead layers at both interfaces has also been neglected.[6,17] Although the rectifying behavior of the devices is clearly observed in both figures, the reverse current in the second case is notably different, being dominated by a conducting phase of the form $I_P = G_P V$, where G_P is a parallel conductance. The origin of this Ohmic component is still unknown but could be related to a local reduction of the SBH at the domain walls close to the Pt/BFO interface caused by the accumulated damage.[5,18] Let us focus the attention on the curve shown in Fig. 2(a). First, we can calculate the SBH modulation from the reverse current as

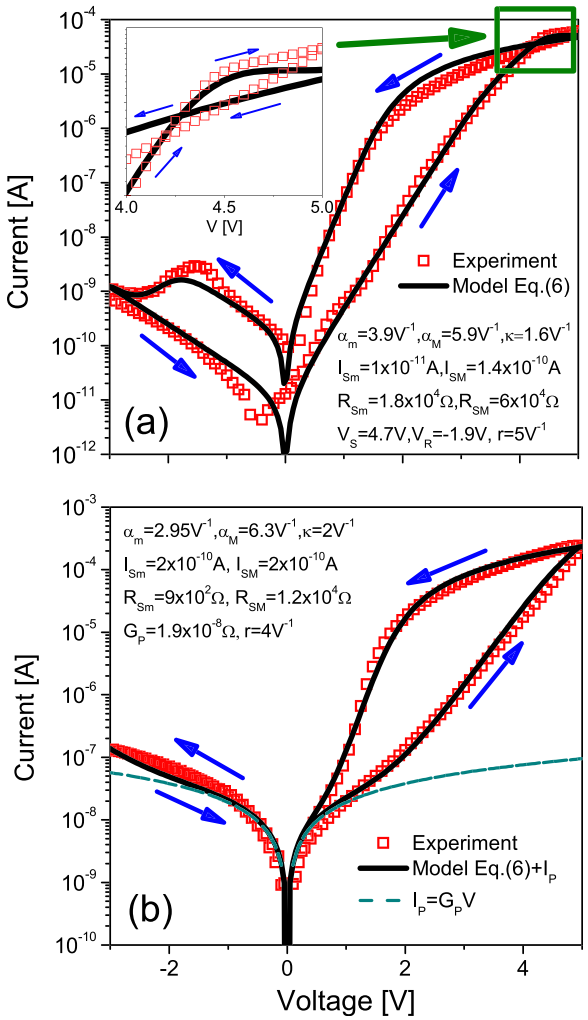

FIG. 2. (a) Experimental (symbols) and simulated (lines) hysteretic I-V loop with polarization reversal effects. (b) Experimental and simulated hysteretic I-V loop with the OFF state affected by a shunt resistance. This case corresponds to a highly cycled device.

$$\Delta\phi = kT\ln(I_{SM}/I_{Sm}), \tag{7}$$

without making any inference about the SBH value itself. Estimated values of $\phi \approx 0.7$–0.8 eV were reported for different Bi-deficient BFO films.[6] For the curve illustrated in Fig. 2(a), $\Delta\phi \approx 0.07$ eV is obtained at room temperature ($kT = 26$ meV) which is far lower than previously published values: 0.6,[1] 1.38,[3] 0.5 eV.[4] Notice that n does not enter into (7) as proposed in Ref. 12. In the case of Fig. 2(b), the value of $\Delta\phi$ extracted from the direct currents is negligible. One frequent problem in determining $\Delta\phi$ is that the diode current for $V < 0$ is often higher than that reported here,[3,9] so that $\Delta\phi$ is calculated indirectly assuming an arbitrary fixed location for the polarization charge (usually 1 nm from the Pt/BFO interface[12]). Moreover, notice that $V_S = 4.7$ V and $V_R = -1.9$ V, which seem to indicate a large asymmetry in the coercive fields for both polarities. Remarkably, $|V_S| - |V_R| = 2.8$ V, which coincides with the BFO band gap ($E_g = 2.8$ eV (Ref. 19)). As a consequence of this asymmetry, the ideality factors ($n = e/\alpha kT$) for the OFF ($n \approx 9.9$) and ON ($n \approx 6.5$) currents, are extremely large and dissimilar (see Fig. 3(a)). We attribute these values to the potential drop V_0 in the BFO/SRO junction, which was not explicitly considered in the previous treatment. We suggest that part of the applied voltage V also drops across this second junction so that a transformation $V \rightarrow V - V_0$ will be assessed next. Since the presence of interfacial layers and the non-equilibrium thermodynamic conditions (because of the current flow) rule out the application of a classical band bending approach based on the solution of the Poisson equation for a ferroelectric semiconductor,[20] we consider instead the semi-empirical voltage correction,[21]

$$V_0(V) = (E_g/2e)\{\tanh[\eta(V-\delta)] + \tanh[\eta\delta]\}, \tag{8}$$

where $E_g = 2.8$ eV is the BFO band gap and $\eta = 0.55\ \mathrm{V}^{-1}$ and $\delta = 2$ V are fitting constants that take into account the formation of the depletion and inversion layers (see the insets in Figs. 3(a) and 3(b)). $\delta = 2$ V corresponds to a moderately p-type doped semiconductor.[4] In this way, as shown in Fig. 3(a), we are able to shift the ON and OFF experimental currents to a lower voltage range so that the only difference in between them solely resides in the SBH modulation effect ($\Delta\phi \approx 0.07$ eV) induced by the polarization reversal. With this voltage correction the asymmetry of the average coercive voltages for both polarities is importantly reduced in consistency with the symmetry of the experimental polarization-electric field (P-E) loops. The resulting lower ideality factor ($n \approx 2.5$) is compatible with the presence of an interfacial layer or with recombination in the depletion region of the BFO layer.[14] Figure 3(c) illustrates the distributions of coercive voltages ($d\lambda/dV$) around V_S and V_R with and without the voltage correction given by Eq. (8). The derivatives of the sigmoidal curves (solid lines) are compared to Gaussian distributions (symbols) located at $V = 4.7$ V and -1.9 V for the original curves and at $V = 2.2$ V and -1.6 V for the corrected curves, all with standard deviation $\sigma = 0.32$ V. The agreement between these two representations supports the idea of a box-type hysteresis loop for the individual domain with normally distributed coercive voltages.[15] Although the asymmetry between V_S and V_R is largely reduced in this way, it is clear that a complete treatment would require a self-consistent solution of the Poisson and current continuity equations across the device. Notice that the proposed model not only can account for the gradual transition from the ON to the OFF state at reverse bias but also the current crossover in the

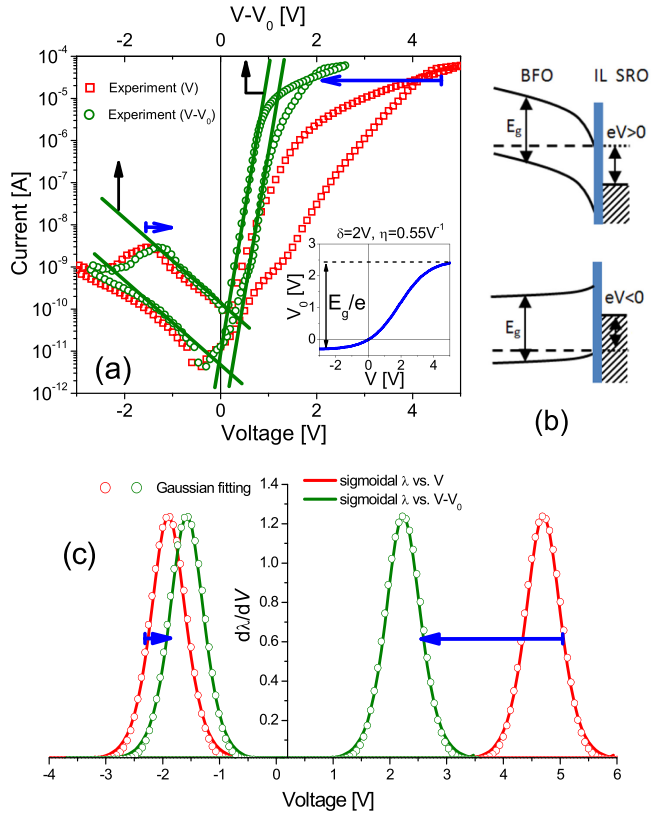

FIG. 3. (a) Modification of the experimental I-V curve using the correction term Eq. (8). The horizontal arrows indicate the shift of the coercive voltages. The inset shows the voltage correction Eq. (8) as a function of the applied bias V. (b) Band bending effect at the BFO/SRO interface for positive and negative biases. (c) Probability distribution ($d\lambda/dV$) of the coercive voltages of the individual domains as a function of the applied voltage V with and without the voltage correction (8) (solid lines). Symbols correspond to fitting results using a Gaussian distribution with standard deviation $\sigma = 0.32$ V.

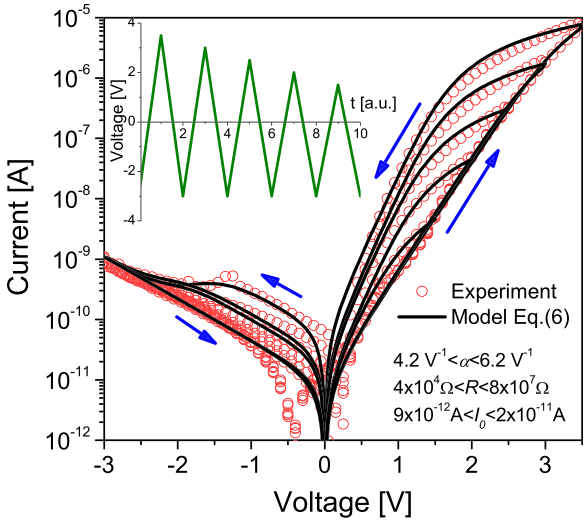

FIG. 4. Experimental (symbols) and simulation results (solid lines) using Eq. (6) for the hysteretic I-V loops. In this case, the device has been subjected to double voltage sweeps starting at -3 V and ending at decreasing maximum voltages from 4 V to 1.5 V. The value of the model parameters is indicated in the figure.

forward bias case (see inset of Fig. 2(a)). This latest feature is not affected by the introduction of (8). Finally, Fig. 4 shows fitting results for the minor *I-V* loops. In this case, double voltage sweeps starting at −3 V with decreasing maximum positive voltage from 4 V to 1.5 V (see inset of Fig. 4) were applied to the device. The maximum voltage is kept below 5 V in order to reduce the damage caused to the structure. Notice that while the OFF state remains constant throughout the experiment indicating a total recovery of the structure after the erasing procedure, the ON state depends on the maximum applied voltage. The agreement between the model results and the experimental data is also very good in this case. Interestingly, it has been recently suggested that these intermediate resistance states can be used to fabricate a multilevel memory device.[7]

In summary, a compact representation of the hysteretic *I-V* characteristics in Pt/BFO/SRO resistive switches using a Schottky diode-like model was presented. The model is based on the solution of the diode equation using the Lambert *W* function. The ON and OFF current states are achieved by means of sigmoidally varying parameters. We showed that modeling the potential distribution across the structure is crucial for the understanding of the device behavior.

This work was supported by the Ministerio de Economía y Competividad of Spain under Project TEC2012-32305 (with funding of the EU under the FEDER program) and by JSPS KAKENHI (No. 26286055), Japan.

[1]D. Lee, S. Baek, T. Kim, J. Yoon, C. Folkman, C. Eom, and T. Noh, Phys. Rev. B **84**, 125305 (2011).
[2]A. Jiang, C. Wang, K. Jin, X. Liu, J. Scott, C. Hwang, T. Tang, H. Lu, and G. Yang, Adv. Mater. **23**, 1277–1281 (2011).
[3]C. Wang, K. Jin, Z. Xu, L. Wang, C. Ge, H. Lu, H. Guo, M. He, and G. Yang, Appl. Phys. Lett. **98**, 192901 (2011).
[4]C. Ge, K. Jin, C. Wang, H. Lu, C. Wang, and G. Yang, Appl. Phys. Lett. **99**, 063509 (2011).
[5]T. Kim, B. Jeon, T. Min, S. Yang, D. Lee, Y. Kim, S. Baek, W. Saenrang, C. Eom, T. Song, J. Yoon, and T. Noh, Adv. Funct. Mater. **22**, 4962–4968 (2012).
[6]A. Tsurumaki, H. Yamada, and A. Sawa, Adv. Funct. Mater. **22**, 1040–1047 (2012).
[7]D. Jiménez, E. Miranda, A. Tsurumaki-Fukuchi, H. Yamada, J. Suñé, and A. Sawa, Appl. Phys. Lett. **103**, 263502 (2013).
[8]S. Hong, T. Choi, J. Jeon, Y. Kim, H. Lee, H. Joo, I. Hwang, J. Kim, S. Kang, S. Kalinin, and B. Park, Adv. Mater. **25**, 2339–2343 (2013).
[9]F. Yan, G. Xing, and L. Li, Appl. Phys. Lett. **104**, 132904 (2014).
[10]Z. Chen, L. He, F. Zhang, J. Jiang, J. Meng, B. Zhao, and A. Jiang, J. Appl. Phys. **113**, 184106 (2013).
[11]T. Choi, S. Lee, Y. Choi, V. Kiryukhin, and S. Cheong, Science **324**, 63 (2009).
[12]W. Wu, J. Guest, Y. Horibe, S. Park, T. Choi, S. Cheong, and M. Bode, Phys. Rev. Lett. **104**, 217601 (2010).
[13]R. Tung, Appl. Phys. Rev. **1**, 011304 (2014).
[14]E. Rhoderick, *Metal-Semiconductor Contacts*, Monographs in Electrical and Electronic Engineering (Oxford University Press, 1980).
[15]D. Laroze, P. Vargas, D. Altbir, and M. Vázquez, Braz. J. Phys. **36**, 908–909 (2006).
[16]A. Ortiz-Conde, F. Garcia-Sánchez, and J. Muci, Solid State Electron. **44**, 1861–1864 (2000).
[17]A. Tsurumaki-Fukuchi, H. Yamada, and A. Sawa, Appl. Phys. Lett. **103**, 152903 (2013).
[18]J. Seidel, L. Martin, Q. He, Q. Zhan, Y. Chu, A. Rother, M. Hawkridge, P. Maksymovych, P. Yu, M. Gajek, N. Balke, S. Kalinin, S. Gemming, F. Wang, G. Catalan, J. Scott, N. Spaldin, J. Orenstein, and R. Ramesh, Nat. Mater. **8**, 229–234 (2009).
[19]S. Clark and J. Robertson, Appl. Phys. Lett. **90**, 132903 (2007).
[20]H. Matsuura, New J. Phys. **2**, 8.1–8.11 (2000).
[21]E. Miranda, S. Kano, C. Dou, J. Suñé, K. Kakushima, and H. Iwai, Appl. Phys. Lett. **101**, 012910 (2012).